Nonlinear Finite Element Analysis of Thick Composite Plates Using Cubic Spline Functions

Ronald L. Hinrichsen* and Anthony N. Palazotto†
Air Force Institute of Technology, Wright-Patterson Air Force Base, Ohio

A nonlinear, thick, composite plate element is developed in which the usual Kirchhoff hypothesis of plane sections remaining plane and undeformed after loading is abandoned. The displacement field is characterized by the sum of displacements with respect to a reference surface and displacements through the thickness. The through-the-thickness deformations are modeled by imposing a cubic spline function and allowing the rotations at interlaminar boundaries to be degrees of freedom in the element. The theory is developed by considering the Lagrangian strains in conjunction with the second Piola-Kirchhoff stress. This formulation leads to a quasi-three-dimensional element that encompasses large displacements with moderately large rotations but is restricted to small strains. Comparisons of linear and nonlinear thick orthotropic plate solutions with those of previously published analytical and numerical results show the validity of the method.

Nomenclature

a	= plate length
a_k	= nodal degrees of freedom
$[A],[B]$	= intermediate integer matrices
$[C]$	$= [A]^{-1}[B]$
C_{ij}	= indicial form of $[C]$
$[D]_j$	= stress-strain matrix for jth layer
$\hat{e}_3$	= unit vector normal to reference surface
$\{e\}$	= physical strain vector
E_1, E_2	= Young's modulus in fiber longitudinal and transverse directions, respectively
G_{ij}	= shear modulus
h	= plate thickness
H_{ji}	= cubic spline shape functions
$[K]$	= elemental stiffness matrix
$[K_0],[K_1],[K_2];$ $[L_0],[L_1],[L_2]$	= linear and nonlinear portions of $[K]$ and $[L]$, respectively
$[L]$	= strain-displacement matrix
M	= number of layers in the laminate
n	= number of nodes in element
N_k	= in-plane elemental shape functions
P_0	= pressure loading magnitude
S	= plate thickness ratio
t_j	= thickness of jth layer
$\boldsymbol{u}$	= displacement vector
$\tilde{\boldsymbol{u}}$	= reference surface displacement vector
$\hat{\boldsymbol{u}}$	= through-the-thickness displacement vector
$(u_1, u_2, u_3),$ $(\tilde{u}_1, \tilde{u}_2, \tilde{u}_3),$ $(\hat{u}_1, \hat{u}_2)$	= components of $\boldsymbol{u}$, $\tilde{\boldsymbol{u}}$, and $\hat{\boldsymbol{u}}$, respectively
$\tilde{u}$	$= \tilde{u}_1$
$\hat{u}$	$= \hat{u}_1$
$\bar{u}, \bar{w}$	= dimensionless displacements
$\{u\}$	= displacement vector
$\tilde{v}$	$= \tilde{u}_2$
$\hat{v}$	$= \hat{u}_2$
w	$= \tilde{u}_3$
$\boldsymbol{x}$	= position vector of a point on the plate reference surface
$\boldsymbol{y}$	= position vector of a point in the plate
(y_1, y_2, y_3)	= coordinates of an orthogonal system
z	$= y_3$ (thickness coordinate)
z_j	= coordinate of the jth layer
$\bar{z}$	= dimensionless thickness coordinate
ϵ_{ij}	= physical strains
$\boldsymbol{\xi}$	= position vector of a point in the plate after deformation
ν_{ij}	= Poisson's ratios
$\bar{\sigma}_x$	= dimensionless direct stress
ϕ_j	$= \partial \hat{u}/\partial z$ at $z = z_j$
θ_j	$= \partial \hat{v}/\partial z$ at $z = z_j$
λ_j	$= t_{j+1}/(t_j + t_{j+1})$
μ_j	$= 1 - \lambda_j$

Presented as Paper 85-0718 at the AIAA/ASME/ASCE/AHS 26th Structures, Structural Dynamics and Materials Conference, Orlando, FL, April 15-17, 1985; received Oct. 24, 1985; revision received March 21, 1986.

*Assistant Professor, Department of Aeronautics and Astronautics.
†Professor, Department of Aeronautics and Astronautics. Associate Fellow AIAA.

Background

FROM the study of the theory of surfaces,[1] one sees that any point on a plate can be located by means of three parameters, two of which vary along a reference surface while the third varies along the reference surface normal. An arbitrary point in the plate is located by means of the position vector

$$\boldsymbol{y}(y_1, y_2, y_3) = \boldsymbol{x}(y_1, y_2) + y_3 \boldsymbol{e}_3(y_1, y_2) \tag{1}$$

where $\boldsymbol{x}$ is the position vector of a corresponding point on the reference surface and y_3 is the distance of the arbitrary point from the reference surface measured along the unit normal $\boldsymbol{e}_3$ (see Fig. 1). Thus, if the plate undergoes a deformation, the arbitrary point moves to a new location $\boldsymbol{\xi}$ and the displacement vector is $\boldsymbol{u}$ as shown in Fig. 1.

The displacement vector is divided into two parts: $\tilde{\boldsymbol{u}}$, a function only of the surface coordinates and associated with the deformation of the reference surface and $\hat{\boldsymbol{u}}$, a function of all three coordinates and associated with the deformation through the thickness. The components of $\boldsymbol{u}$ can be written as

$$u_1 = \tilde{u}_1(y_1, y_2) + \hat{u}_1(y_1, y_2, y_3) \tag{2}$$

$$u_2 = \tilde{u}_2(y_1, y_2) + \hat{u}_2(y_1, y_2, y_3) \tag{3}$$

$$u_3 = \tilde{u}_3(y_1, y_2) \tag{4}$$

Under such a deformation, the Lagrangian strains are derived. Although this paper deals specifically with flat-plate structures, the full derivation for a general curved structure was carried out in Ref. 2.

If one converts from tensorial to physical strain, one obtains[2]

$$\epsilon_{11} = (\tilde{u}_1 + \hat{u}_1)_{,1} + \tfrac{1}{2}\left\{[(\tilde{u}_1 + \hat{u}_1)_{,1}]^2 + [(\tilde{u}_2 + \hat{u}_2)_{,1}]^2 + (\tilde{u}_{3,1})^2\right\} \quad (5)$$

$$\epsilon_{22} = (\tilde{u}_2 + \hat{u}_2)_{,2} + \tfrac{1}{2}\left\{[(\tilde{u}_1 + \hat{u}_1)_{,2}]^2 + [(\tilde{u}_2 + \hat{u}_2)_{,2}]^2 + (\tilde{u}_{3,2})^2\right\} \quad (6)$$

$$\epsilon_{33} = \tilde{u}_{3,3} + \tfrac{1}{2}\left\{(\hat{u}_{1,3})^2 + (\hat{u}_{2,3})^2 + (\tilde{u}_{3,3})^2\right\} \quad (7)$$

$$2\epsilon_{23} = \hat{u}_{2,3} + \tilde{u}_{3,2} + \hat{u}_{1,3}(\tilde{u}_1 + \hat{u}_1)_{,2} + \hat{u}_{2,3}(\tilde{u}_2 + \hat{u}_2)_{,2} + \tilde{u}_{3,3}\tilde{u}_{3,2} \quad (8)$$

$$2\epsilon_{13} = \hat{u}_{1,3} + \tilde{u}_{3,1} + \hat{u}_{1,3}(\tilde{u}_1 + \hat{u}_1)_{,1} + \hat{u}_{2,3}(\tilde{u}_2 + \hat{u}_2)_{,1} + \hat{u}_{3,3}\tilde{u}_{3,1} \quad (9)$$

$$2\epsilon_{12} = (\tilde{u}_1 + \hat{u}_1)_{,2} + (\tilde{u}_2 + \hat{u}_2)_{,1} + (\tilde{u}_1 + \hat{u}_1)_{,2}(\tilde{u}_1 + \hat{u}_1)_{,1} + (\tilde{u}_2 + \hat{u}_2)_{,1}(\tilde{u}_2 + \hat{u}_2)_{,2} + \tilde{u}_{3,2}\tilde{u}_{3,1} \quad (10)$$

where $(\ )_{,i}$ represents differentiation. In this form, the equations show some new terms $\hat{u}_{i,j}$ and their products with the other displacements.

These strain-displacement relations can be written in vector form as

$$\{e\} = [L]\{u\} \quad (11)$$

where

$$\{e\} = [\epsilon_{11}, \epsilon_{22}, \epsilon_{33}, 2\epsilon_{23}, 2\epsilon_{13}, 2\epsilon_{12}]^T \quad (12)$$

and

$$\{u\} = \begin{Bmatrix} \tilde{u}_1 + \hat{u}_1 \\ \tilde{u}_2 + \hat{u}_2 \\ \tilde{u}_3 \end{Bmatrix} = \begin{Bmatrix} \tilde{u} + \hat{u} \\ \tilde{v} + \hat{v} \\ w \end{Bmatrix} = \begin{Bmatrix} u \\ v \\ w \end{Bmatrix} \quad (13)$$

The matrix $[L]$ is a nonlinear differential operator that can be further reduced to linear and nonlinear parts:

$$[L] = [L_0] + [L_1] + [L_2] \quad (14)$$

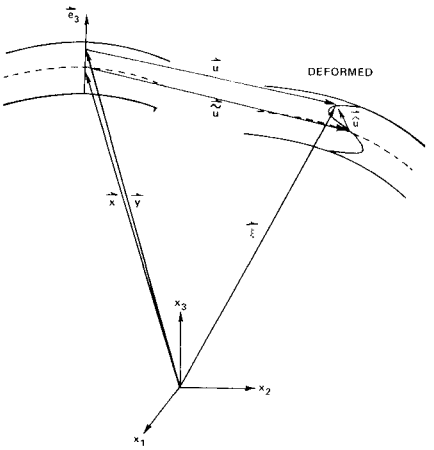

Fig. 1 Deformation terms and geometry.

where $[L_0]$ contains only linear differential operators, $[L_1]$ nonlinear expressions involving only the reference surface displacements, and $[L_2]$ nonlinear expressions involving the through-the-thickness displacements.

The Finite Element

Consider a plate made up of M orthotropic laminae, each having its own set of material properties, which may vary from layer to layer (see Fig. 2). Let the reference surface be chosen to be the bottom-most layer, i.e., $z = z_0$. Then the reference surface displacements $(\tilde{u}, \tilde{v}, w)$ can be modeled using a two-dimensional isoparametric element. The through-the-thickness displacements $(\hat{u}, \hat{v})$ are represented by means of a cubic spline as follows:

Let the bottom of the jth layer be given the coordinate z_{j-1} and the top z_j, where $z = y_3$. At $z = z_{j-1}$, let $\partial\hat{u}/\partial z = \phi_{j-1}$ and, at $z = z_j$, let $\partial\hat{u}/\partial z = \phi_j$. Then a cubic spline is formed to represent the displacement $\hat{u}(z)$. That is,

$$\hat{u}_j(z) = \phi_{j-1}\frac{(z_j - z)^2(z - z_{j-1})}{t_j^2} - \phi_j\frac{(z - z_{j-1})^2(z_j - z)}{t_j^2} + \hat{u}_{j-1}\frac{(z_j - z)^2[2(z - z_{j-1}) + t_j]}{t_j^3} + \hat{u}_j\frac{(z - z_{j-1})^2[2(z_j - z) + t_j]}{t_j^3} \quad (15)$$

with the continuity requirement

$$\lambda_j\phi_{j-1} + 2\phi_j + \mu_j\phi_{j+1} = 3\lambda_j\frac{\hat{u}_j - \hat{u}_{j-1}}{t_j} + 3\mu_j\frac{\hat{u}_{j+1} - \hat{u}_j}{t_{j+1}} \quad (16)$$

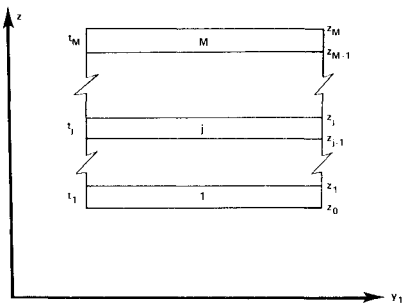

Fig. 2 Typical laminate plate lay-up.

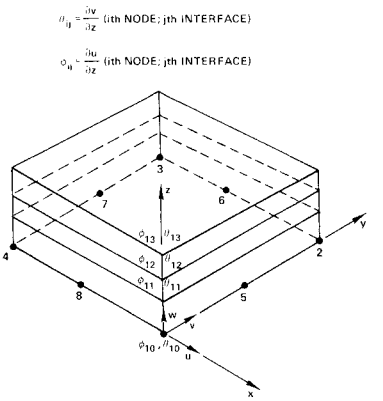

Fig. 3 The 8-noded element.

where

$$\hat{u}_j(z) = \text{restriction of } \hat{u} \text{ to } j\text{th layer} \tag{17}$$

$$t_j = z_j - z_{j-1} \tag{18}$$

$$\lambda_j = t_{j+1}/(t_j + t_{j+1}) \tag{19}$$

$$\mu_j = 1 - \lambda_j \tag{20}$$

Equation (16) is the well-known continuity requirement in spline theory.[3] It is a system of linear equations.

If each of the laminae has equal thickness t, then the system of equations in Eq. (16) takes the form

$$[B]\{\phi\} = 3/t[A]\{\hat{u}\} \tag{21}$$

where

$$\{\phi\} = [\phi_0 \quad \phi_1 \quad \phi_2 \cdots \phi_M]^T \tag{22}$$

$$\{\hat{u}\} = [\hat{u}_0 \quad \hat{u}_1 \ldots \hat{u}_M]^T \tag{23}$$

$[B]$ and $[A]$ are matrices whose components are integer numbers and $\hat{u}_0 = 0$. The system is solved to yield

$$\{\hat{u}\} = t/3[C]\{\phi\} \tag{24}$$

where

$$[C] = [A]^{-1}[B] \tag{25}$$

The values of $\{\hat{u}\}$ are then substituted into Eq. (15) to yield a cubic spline that is a function of the rotations $\{\phi\}$. Upon rearranging, Eq. (15) can be written as

$$\hat{u}_j(z) = \sum_{i=1}^{M+1} H_{ji}\phi_{i-1} \tag{26}$$

where

$$H_{ji} = \left\{ \delta_{ij}\frac{(z_j - z)^2(z - z_{j-1})}{t^2} - \delta_{i-1,j}\frac{(z - z_{j-1})^2(z_j - z)}{t^2} + C_{j-1,i}\frac{(z_j - z)^2[2(z - z_{j-1}) + t]}{3t^2} + C_{ji}\frac{(z - z_{j-1})^2[2(z_j - z) + t]}{3t^2} \right\} \tag{27}$$

δ_{ij} is Kronecker's delta and $C_{0i} = 0$.

In this form, the H_{ji} can be thought of as a set of global shape functions to represent displacements in the z direction.

If one turns attention to the $\hat{v}$ component of displacement and makes the same assumptions and arguments as were made for $\hat{u}$, one would obtain expressions for H_{ji} that are identical to those already obtained. The $\hat{v}$ displacement is then written as

$$\hat{v}_j(z) = \sum_{i=1}^{M+1} H_{ji}\theta_{i-1} \tag{28}$$

where

$$\theta_{i-1} = \partial\hat{v}/\partial z|_{z=z_{i-1}} \tag{29}$$

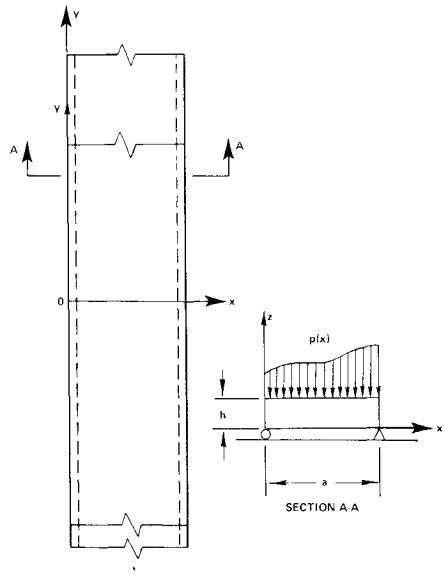

Fig. 4 The plate strip problem.

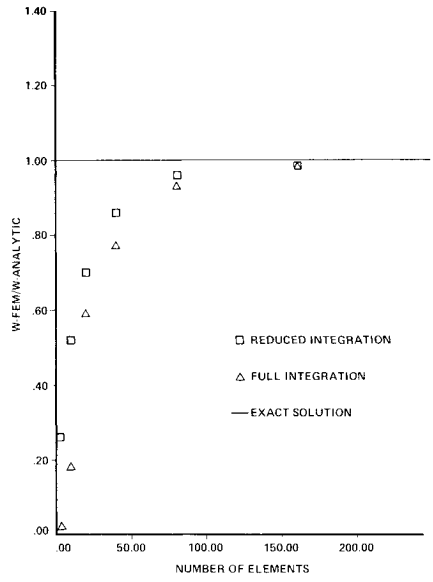

Fig. 5 Convergence of the 3-node element.

Using the isoparametric elemental[4] shape functions N_k for the in-plane distributions, we can write the following:

$$\phi_{i-1}(x, y) = \sum_{k=1}^{n} N_k\phi_{ki-1} \tag{30}$$

$$\theta_{i-1}(x, y) = \sum_{k=1}^{n} N_k\theta_{ki-1} \tag{31}$$

$$\hat{u}(x, y, z) = \sum_{k=1}^{n}\sum_{i=1}^{M+1} H_{ji}N_k\phi_{ki-1} \tag{32}$$

$$\hat{v}(x, y, z) = \sum_{k=1}^{n}\sum_{i=1}^{M+1} H_{ji}N_k\theta_{ki-1} \tag{33}$$

where ϕ_{ki-1} and θ_{ki-1} are $\partial\hat{u}/\partial z$ and $\partial\hat{v}/\partial z$ evaluated at the kth node, $(i-1)$st interlaminar boundary, and n is the number of nodes on the element.

The reference surface displacements are also distributed using the shape functions N_k; thus,

$$\tilde{u}(x,y) = \sum_{k=1}^{n} N_k \tilde{u}_k \tag{34}$$

$$\tilde{v}(x,y) = \sum_{k=1}^{n} N_k \tilde{v}_k \tag{35}$$

$$w(x,y) = \sum_{k=1}^{n} N_k w_k \tag{36}$$

To obtain the full expression for the displacements u and v within the element, the contributions of $\tilde{u}$ must be added to $\hat{u}$, and $\tilde{v}$ added to $\hat{v}$. If the vector of nodal unknowns is defined as

$$\{a_k\} = [\tilde{u}_k, \phi_{k0} \dots \phi_{kM}, \tilde{v}_k, \theta_{k0} \dots \theta_{kM}, w_k]^T \tag{37}$$

for node k (see Fig. 3), then the shape function matrix associated with a_k becomes

$$[N_k] = \begin{bmatrix} N_k & 0 & 0 \\ H_{j1}N_k & 0 & 0 \\ \vdots & \vdots & \vdots \\ H_{jM}N_k & 0 & 0 \\ 0 & N_k & 0 \\ 0 & H_{j1}N_k & 0 \\ \vdots & \vdots & \vdots \\ 0 & H_{jM}N_k & 0 \\ 0 & 0 & N_k \end{bmatrix}^T \tag{38}$$

The displacements at the kth node would be

$$u_k = \begin{Bmatrix} \tilde{u}+\hat{u} \\ \tilde{v}+\hat{v} \\ w \end{Bmatrix}_k = \{N_k\}\{a_k\} \tag{39}$$

Thus, the elemental displacements can be written as

$$\{u\} = [N]\{a\} \tag{40}$$

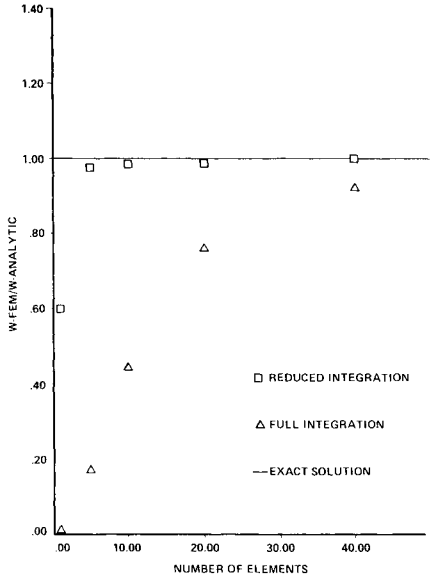

Fig. 6 Convergence of the 4-node element.

and the elemental strains are

$$\{e\} = [L]\{u\} = [L][N]\{a\} \tag{41}$$

With this strain-displacement relation and stress-strain relations for each of the laminae, the elemental equations are readily derived using one of the variational principles.

The elemental stiffness matrix obtained is

$$[K] = \sum_{j=1}^{M} \iiint_{\text{Vol}} \left[[N]^T[L]^T[D][L][N]\,dv\right]_j \tag{42}$$

where the summation is over each of the M laminae; the integration is over the jth laminae.

Since $[L]$ is composed of its linear and nonlinear parts, $[L_0],[L_1],[L_2]$, the stiffness matrix is readily expressed as

$$[K] = [K_0] + [K_1] + [K_2] \tag{43}$$

where

$$[K_0] = \sum_{j=1}^{M} \iiint_{\text{Vol}} \left\{[N]^T[L_0]^T[D][L_0][N]\right\}_j dv \tag{44}$$

$$\begin{aligned}[K_1] = \sum_{j=1}^{M} \iiint_{\text{Vol}} \big\{&[N]^T[L_0]^T[D][L_1][N] \\ &+[N]^T[L_1]^T[D][L_0][N] \\ &+[N]^T[L_1]^T[D][L_1][N]\big\}_j dv\end{aligned} \tag{45}$$

$$\begin{aligned}[K_2] = \sum_{j=1}^{M} \iiint_{\text{Vol}} \big\{&[N]^T[L_0]^T[D][L_2][N] \\ &+[N]^T[L_2]^T[D][L_0][N] \\ &+[N]^T[L_1]^T[D][L_2][N] \\ &+[N]^T[L_2]^T[D][L_1][N] \\ &+[N]^T[L_2]^T[D][L_2][N]\big\}_j dv\end{aligned} \tag{46}$$

where, for arbitrary fiber orientation within the jth layer,

$$[D]_j = \begin{bmatrix} D_{11} & D_{12} & D_{13} & 0 & 0 & D_{16} \\ & D_{22} & D_{23} & 0 & 0 & D_{26} \\ & & D_{33} & 0 & 0 & D_{36} \\ \text{SYM} & & & D_{44} & D_{45} & 0 \\ & & & & D_{55} & 0 \\ & & & & & D_{66} \end{bmatrix}_j \tag{47}$$

Results

A finite element program was written to incorporate the notions of the preceding sections. A family of two-dimensional isoparametric elements (ranging from the 3-noded triangle to the 8-noded serendipity quadrilateral element) was implemented in the program. The integrations were performed numerically using Gauss-Legendre quadrature. The solutions of the linear problems were carried out on a CDC Cyber 175, using the Crout variation of Gauss elimination. The nonlinear problems were solved on the Cyber using the modified Newton-Raphson technique.[5] Before solving any physical problem, a check of the eigenvalues and eigenvectors of $[K_0]$ was performed to determine the element's qualities. Essentially, the results of this check were favorable. The rigid body modes associated with the 3-, 4-, and 8-noded two-dimen-

sional elements were reproduced using exact integration in-plane.

The authors have carried out the solutions to four problems in order to show the range and applicability of the newly developed element in solving linear and nonlinear plate problems. It should be pointed out that the extension of element use into shell application has not been attempted but, as will be shown subsequently, the characteristics of this new element are favorable for such an extension.

The first application examined is that of the plate strip (see Fig. 4). The strip is infinitely long in the y direction, simply supported, and loaded uniformly in the lateral direction so as to cause cylindrical bending. That is, the lateral displacements w are symmetric about the centerline of the strip and are independent of y. The displacements v in the y direction are zero. The strip consisted of two laminae whose fibers were oriented at 0 deg with respect to the x axis. The loading intensity was $P_0 = 163.84$ psi, and the material properties were $E_1 = 2.5 \times 10^7$ psi, $E_2 = 1.0 \times 10^6$ psi, $\nu_{12} = 0.25$, $G_{12} = 5.0 \times 10^6$ psi, $G_{13} = 5.0 \times 10^6$ psi, $G_{23} = 2.0 \times 10^6$ psi, $h = 0.2$ in., and $a = 10.0$ in. The analytical solution for this problem was determined from Fourier analysis (using Navier's method)[6] to be

$$W_{\max} = \frac{4P_0 a^4}{\pi^5 D} \sum_{m=1}^{\infty} \frac{1}{m^5} \sin\left(\frac{m\pi}{2}\right) \quad (m = 1,3,5\ldots) \quad (48)$$

where

$$D = Q_{11} h^3/12 \quad (49)$$

$$Q_{11} = E_1^2/\left[E_1 - \nu_{12}^2 E_2\right] \quad (50)$$

The modeling for the problem was to take a thin slice of the plate, exploit the centerline symmetry, and impose the $v = 0$ and $v_{,2} = 0$ boundary conditions on the slice edges. The slice was then discretized into elements, and a convergence study carried out.

Figures 5-7 show the results of the study for the 3-, 4-, and 8-noded elements, respectively. Note that full and reduced integration schemes were used with each element. In each case, the reduced integration scheme converged more rapidly than the full integration scheme. In the cases of the 3- and 4-noded elements using full integration, the convergence to the analytical solution was obtained only when the dimensions of the element were reduced to about one-third of the plate thickness. In a subsequent paragraph, the phenomenon relating to a thin isotropic plate and associated locking[7] will be discussed. This phenomenon is closely associated with the difficulties alluded to here for the full integration technique on the orthotropic problem.

The second problem presented is the plate strip solved analytically by Pagano[8] for various ply orientations and thicknesses. This problem is geometrically identical to the previous one, but the loading is sinusoidal in nature. That is,

$$p(x) = p_0 \sin(\pi x/a) \quad (51)$$

$$p_0 = 162.755 \text{ psi} \quad (52)$$

The plate was modeled by using five 8-noded rectangles and reduced integration. Figures 8 and 9 show the good agreement of the element with Pagano's results for various thicknesses and ply orientations. In these figures,

$$\bar{w} = \left(100 E_2 h^3/P_0 a^4\right) w_{\max} \quad (53)$$

$$S = a/h \quad (54)$$

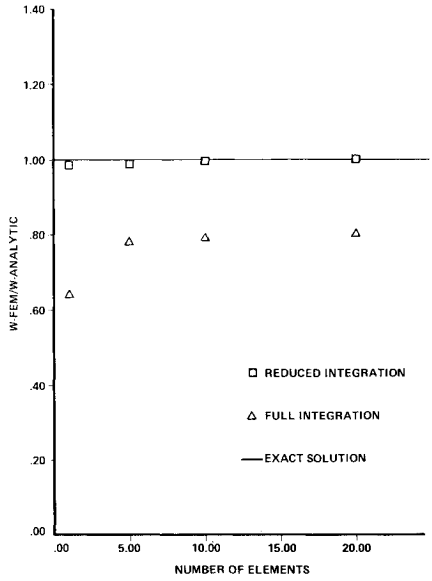

Fig. 7 Convergence of the 8-node element.

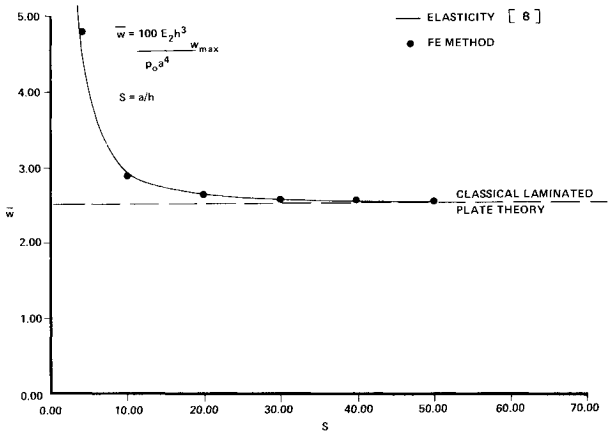

Fig. 8 S vs $\bar{w}$ for fibers oriented at (0°, 90°).

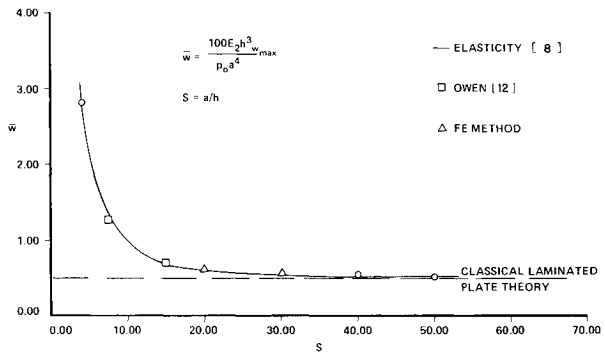

Fig. 9 S vs $\bar{w}$ for fibers oriented at (0°, 90°, 0°).

Figures 10 and 11 show plots of $\bar{u}$ vs $\bar{z}$ for very thick plates at $x = 0$, where

$$\bar{u} = E_2 u/hp_0 \quad (55)$$

and

$$\bar{z} = z/h \quad (56)$$

Plots of $\bar{\sigma}_x$ vs $\bar{z}$ are presented in Figs. 12 and 13. Note that, in each of these figures, the finite element follows very closely the results obtained by Pagano.[8]

The third problem presented is that of the four-ply (0°, 90°, 90°, 0°) square plate simply supported along each of its edges and subjected to a transverse load of the form

$$p = p_0 \sin(\pi x/a)\sin(\pi y/a) \tag{57}$$

The plate was modeled using twenty-five 8-noded elements for the quarter plate and reduced integration.

Figure 14 shows a comparison of $\bar{w}$ vs S for the plate. Results obtained by the present method compare favorably with the known solution and appear to be more accurate than those obtained by Pryor and Barker.[9] The solution of each of the above problems with isotropic material properties was also performed. Difficulties were encountered in solving the thin isotropic cases. A review of the literature[13,14] shows that this failure of the "thick-plate" element to converge to the "thin-plate" solution is common. These thick-plate theories are essentially of the Mindlin type, where the normal to a reference surface before deformation remains straight but not necessarily normal after deformation. These assumptions lead to stiffness matrices that characterize bending independent of the transverse shear effects. The difficulty encountered by these elements as the plate becomes thin is that the shear stiffness matrix remains too stiff. Normally, this is looked upon as a "penalty," and a number of techniques have been formulated that attempt to reduce the penalty. The methods of penalty reduction involve reduced or selective integration or formulation of a penalty function that is essentially a multiplier on the shear stiffness matrix, which approaches zero as the plate thickness is reduced. The failure of the thick plate element to converge to the thin-plate solution has been attributed to the "locking" phenomenon.

The present formulation is not of the Mindlin type since reference surface normals are allowed to deform after loading. Furthermore, the derivation of the stiffness matrix is carried out from an elasticity point of view. The stiffness matrix is not characterized by a bending part and a shear part.

The thin-plate solution is a result of Kirchhoff's hypotheses, which neglect both the direct strain ϵ_z and the shear strains γ_{xz}, γ_{yz}. In addition, the normal stress is assumed small compared to σ_x and σ_y so that it is neglected in the stress-strain relations. These assumptions lead to a theory based only on the transverse displacement w. In the present work, the direct transverse strain is neglected, but the shear strains are not. The problem is not reduced as is the classical thin-plate problem. The effects of the transverse shear terms are always present.

An attempt was made to find a method for reducing the effects brought about by the shear strains. The method arrived at was to lower the magnitudes of the shear moduli G_{13} and G_{23}. This reduction resulted in a softening of the element and a convergence to the thin-plate solution.

Looking back at the locking problem and methods that have been used to eliminate the locking, one sees that in each case there was an attempt to soften the element in some way so as to eliminate the effects of transverse shear. In effect, what was being done was to artificially reduce the effects of G_{13} and G_{23} on the solution of the problem. The present work takes a less artificial and more direct approach to the problem. Since the element was designed for a thick structure, the three-dimensional effects had to be considered. Direct transverse stress and transverse shear strains were always considered. The only way to reduce their effects was through the constitutive relation $[D]$.

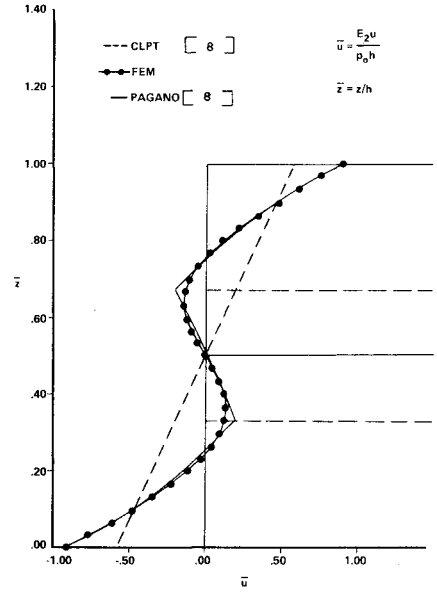

Fig. 11 $\bar{u}$ vs $\bar{z}$ for fibers oriented at (0°, 90°, 0°)-sym = 4.

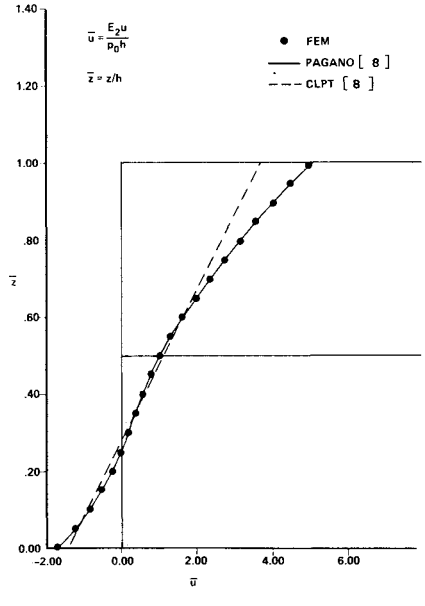

Fig. 10 $\bar{u}$ vs $\bar{z}$ for fibers oriented at (0°, 90°)-sym = 4.

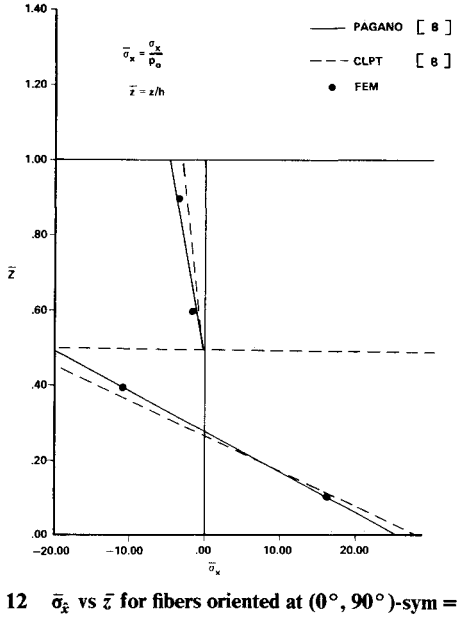

Fig. 12 $\bar{\sigma}_{\bar{x}}$ vs $\bar{z}$ for fibers oriented at (0°, 90°)-sym = 4.

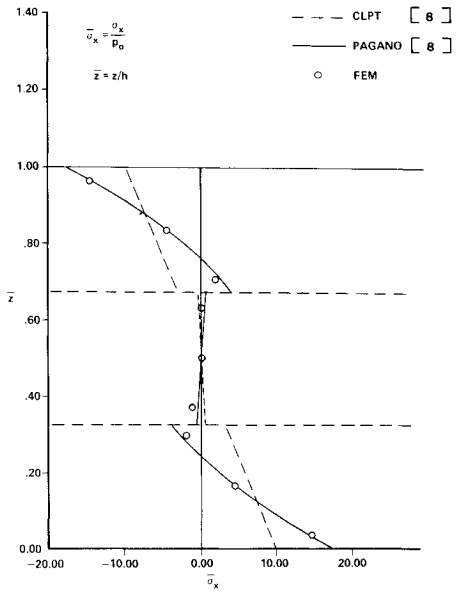

Fig. 13 $\bar{\sigma}_x$ vs $\bar{z}$ for fibers oriented at (0°, 90°, 0°)-sym = 4.

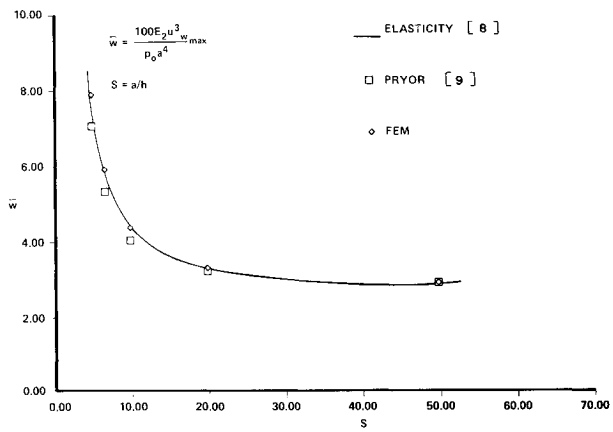

Fig. 14 S vs $\bar{w}$ for square plate (0°, 90°, 90°, 0°).

The fourth and final problem presented herein is a square orthotropic (0°,0°) plate loaded transversely with a uniformly distributed load $p = p_0$. The boundaries of the plate were clamped, and the quarter plate was modeled using sixteen 4-noded elements with reduced integration. This problem was chosen as a check of how the inclusion of the nonlinear terms of the theory would affect the solution. The check was made by proportionally increasing the load p and observing the transverse deflection w at the center of the plate where it was maximum. Figure 15 shows a plot of the results obtained. This plot gives a comparison between the present element, a similar element developed by Witt,[10] and an approximate analytical solution obtained by Chia.[11] Note in particular that the inclusion of the $[K_1]$ terms gives results that are nearly identical to those obtained by Chia, who used a perturbation method on the von Kármán plate equations. The inclusion of the higher-order thickness terms of $[K_2]$ yields an expected softening of the element as the loads are increased.

The inclusion of the $[K_2]$ terms in the nonlinear formulation is an advance in the state-of-the-art in through-the-thickness representations. It is seen to become more important as load levels are increased (assuming yield stress is not exceeded). Since $[K_2]$ contains nonlinear transverse rotational terms, it would also become more important whenever transverse shear terms affect the problem. The thicker the structure, the more important the inclusion of these terms becomes.

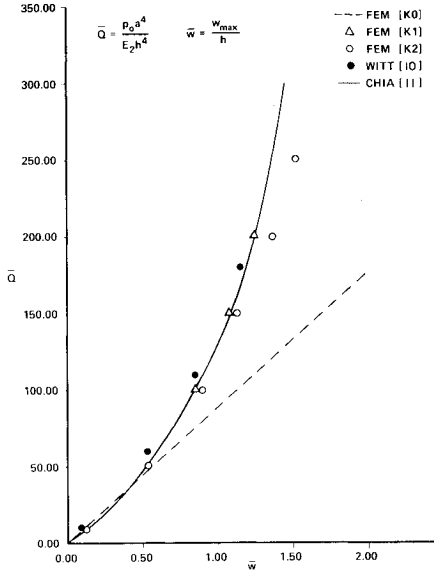

Fig. 15 $\bar{Q}$ vs $\bar{w}$ for nonlinear square plate.

Conclusions

We have presented a theory and finite element that have been shown to be accurate for a class of thin and thick orthotropic plate problems.

The element shows favorable interelement strain compatibility through the thickness. In applications to thick plates where three-dimensional brick elements are normally used, the present element shows a favorable reduction in nodal degrees of freedom from $5M + 5$ to $2M + 5$, where M is the number of plies. In addition, the inclusion of the nonlinear through-the-thickness terms of $[K_2]$ in plate analysis leads to a solution that is "softer" than the $[K_1]$ solution.

References

[1] Saada, A.S., *Elasticity Theory and Applications*, Pergamon Press Inc., Elmsford, NY, 1974.

[2] Hinrichsen, R.L., "The Nonlinear Analysis of Thick Composite Plates Using a Cubic Spline Function," Ph.D. Dissertation, Air Force Institute of Technology, Wright-Patterson AFB, OH, 1984.

[3] Ahlberg, J.H., Nilson, E.N., and Walsh, J.L., *The Theory of Splines and Their Applications*, Academic Press, Orlando, FL, 1967.

[4] Reddy, J.N., *An Introduction to the Finite Element Method*, McGraw-Hill Book Co., New York, 1984.

[5] Zienkiewicz, O.C., *The Finite Element Method*, 3rd ed., McGraw-Hill Book Co., London, 1977.

[6] Szilard, R., *Theory and Analysis of Plates—Classical and Numerical Methods*, Prentice-Hall, Englewood Cliffs, NJ, 1974.

[7] Cook, R.D., *Concepts and Applications of Finite Element Analysis*, 2nd ed., John Wiley & Sons, New York, 1981.

[8] Pagano, N.J., "Exact Solutions for Composite Laminates in Cylindrical Bending," *Journal of Composite Materials*, Vol. 3, July 1969, pp. 398-411.

[9] Pryor, C.W., Jr. and Barker, R.M., "A Finite Element Analysis Including Transverse Shear Effects for Applications to Laminate Plates," *AIAA Journal*, Vol. 9, May 1971, pp. 912-917.

[10] Witt, W., "Formulation of a Nonlinear Compatible Finite Element for the Analysis of Laminated Composites," Ph.D. Dissertation, Air Force Institute of Technology, Wright-Patterson AFB, OH, 1983.

[11] Chia, C-Y, "Large Deflection of Rectangular Orthotropic Plates," *Journal of the Engineering Mechanics Division ASCE*, Vol. 98, EM5, 1972.

[12] Owen, D.R.J. and Figueiras, J.A., "Anisotropic Elasto-Plastic Finite Element Analysis of Thick and Thin Plates and Shells," *International Journal for Numerical Methods in Engineering*, Vol. 19, 1983, pp. 541-566.

[13] Pugh, E.D.L., Hinton, E., and Zienkiewicz, O.C., "A Study of Quadrilateral Plate Bending Elements With Reduced Integration," *International Journal for Numerical Methods in Engineering*, Vol. 12, 1978, pp. 1059-1079.

[14] Hughes, T.J.R., Cohen, M., and Haroun, M., "Reduced and Selective Integration Techniques in the F.E. Analysis of Plates," *Nuclear Engineering Design*, Vol. 46, 1978, pp. 203-222.